THE JOURNAL OF BIOLOGICAL CHEMISTRY

Vol. 263, No. 7, Issue of March 5, pp. 3256-3260, 1988
Printed in U.S.A.

The Binding of L-Valyl-L-tryptophan to Crystalline Thermolysin Illustrates the Mode of Interaction of a Product of Peptide Hydrolysis*

(Received for publication, August 4, 1987)

Hazel M. Holden‡ and Brian W. Matthews§

From the Institute of Molecular Biology and Department of Physics, University of Oregon, Eugene, Oregon 97403

Crystallographic analysis of the binding of mercaptoacetyl-L-valyl-L-tryptophan to thermolysin suggests that this inhibitor is hydrolyzed by the crystalline enzyme. The apparent product of hydrolysis, L-valyl-L-tryptophan (Val-Trp), occupies the S_1'-S_2' subsites of the active site, not the S_1-S_1' subsites as observed previously for the dipeptide L-alanyl-L-phenylalanine (Ala-Phe). The difference in binding of Val-Trp and Ala-Phe is consistent with the specificity requirements and preferences of thermolysin. The binding of Val-Trp illustrates the mode of interaction of one of the products of peptide hydrolysis. High resolution crystallographic refinement indicates that the valyl amino group makes three hydrogen bonds to the enzyme and to solvent and, in addition, is 2.8 Å from the carboxylate of Glu-143. This is the first instance in which a direct interaction has been observed between Glu-143 and the scissile nitrogen. As such, the study directly supports the mechanism of action for thermolysin proposed by Hangauer *et al.* (Hangauer, D. G., Monzingo, A. F., and Matthews, B. W. (1984) *Biochemistry* 23, 5730-5741) and, by analogy, indirectly supports the similar mechanism proposed for carboxypeptidase A (Monzingo, A. F., and Matthews, B. W. (1984) *Biochemistry* 23, 5724-5729).

Thermolysin is a thermostable metalloendopeptidase of 34,600 daltons molecular mass isolated from *Bacillus thermoproteolyticus*. Its three-dimensional structure has no resemblance to that of carboxypeptidase A, but the active sites of these two Zn(II) metalloenzymes have elements in common (1). Based on previous crystallographic and model-building analyses a common mechanism of action was proposed for the two enzymes (2, 3). For thermolysin, the suggested mechanism has been shown to be consistent with subsequent structural analyses of presumed transition-state analogues (4, 5). In the case of carboxypeptidase A, the postulated mechanism has received strong support from site-directed mutagenesis (6) and has recently been adopted by Lipscomb and coworkers (7) to rationalize the binding of substrate analogues to the crystalline enzyme.

Early structural studies of thermolysin (8) showed that the dipeptide L-alanyl-L-phenylalanine and the dipeptide analogue β-phenylpropionyl-L-phenylalanine occupy the S_1 and S_1' subsites (9) of the thermolysin active site cleft with the carbonyl oxygen of the peptide bond liganded to the zinc. In this report it is shown that the dipeptide L-valyl-L-tryptophan (hereafter Val-Trp) does not straddle the zinc. Rather, the inhibitor occupies the S_1' and S_2' subsites. As such, Val-Trp is a model for the product of peptide cleavage on the COOH-terminal side of the scissile bond. The observed mode of binding is consistent with one of the key features of the postulated mechanism of action, namely that Glu-143 of thermolysin (or Glu-270 of carboxypeptidase A) acts as a "proton shuttle," transferring a proton from the attacking water molecule to the leaving nitrogen of the cleaved substrate (2, 3).

This study was not begun as an analysis of Val-Trp *per se*. Rather, it had its origins in an analysis of the binding of peptide mercaptans to thermolysin. It had previously been shown that a mercaptopropanoyl dipeptide inhibitor bound to thermolysin with the sulfur liganded to the zinc (10) as anticipated by Ondetti and co-workers (*e.g.* see Ref. 11). Dr. M. A. Ondetti proposed to us that mercaptoacetyl dipeptides, known to be good inhibitors of the zinc peptidases (12, 13), might bind to thermolysin in a bidentate manner with both the sulfur and the acetyl oxygen liganded to the zinc. To test this hypothesis, Dr. Ondetti provided us with a sample of mercaptoacetyl-L-valyl-L-tryptophan (HSAc-Val-Trp).[1] A detailed crystallographic analysis of the binding of this compound (see below) showed clear electron density for the Val-Trp portion of the inhibitor, but not for the mercaptoacetyl moiety. The simplest interpretation of this result is that the inhibitor was hydrolyzed in the presence of the crystalline enzyme during soaking and x-ray data collection (about 3 weeks). This is also supported by experiments in which Val-Leu was bound to crystalline thermolysin and found to give results apparently identical with the binding of HSAc-Val-Trp.

EXPERIMENTAL PROCEDURES

Mercaptoacetyl-L-valyl-L-tryptophan, a kind gift of M. A. Ondetti, Squibb Institute for Medical Research, was dissolved in a standard mother liquor of 10 mM calcium acetate, 10 mM Tris, 7% (v/v) dimethyl sulfoxide, pH 7.2, and its binding to crystalline thermolysin was monitored by measuring (0*kl*) projection x-ray data (*cf.* Ref. 14). Projection maps indicated that the inhibitor was bound in the active site region but showed no electron density at the expected location of the electron-dense sulfur atom (see discussion below). A full three-dimensional data set to 1.7-Å resolution was collected by oscillation photography (15) from a thermolysin crystal soaked, prior to data collection, for 14 days in the presence of 10 mM inhibitor and 5 mM dithiothreitol.

Binding of the inhibitor was visualized by calculating electron

* This work was supported in part by Grant GM20066 from the National Institutes of Health, Grant DMB8611084 from the National Science Foundation, and by the M. J. Murdock Charitable Trust. The costs of publication of this article were defrayed in part by the payment of page charges. This article must therefore be hereby marked "*advertisement*" in accordance with 18 U.S.C. Section 1734 solely to indicate this fact.

‡ Supported in part by Fellowship DRG-667 of the Damon Runyon-Walter Winchell Cancer Fund. Present address: Dept. of Biochemistry, Biological Sciences West, University of Arizona, Tucson, AZ 85721.

§ To whom correspondence should be sent.

[1] The abbreviation used is: HSAc, mercaptoacetyl.

density maps with coefficients of the form ($F_{complex} - F_{native}$) and ($2F_{complex} - F_{native}$). Initial coordinates (for the Val-Trp portion of the inhibitor) were obtained using the program FRODO (16) on an Evans and Sutherland PS300 graphics system. Coordinates of the protein-inhibitor complex were refined using the restrained least-squares "TNT" package (17) of programs.

RESULTS

Summaries of the x-ray data collection and refinement statistics for the complex of thermolysin with HSAc-Val-Trp are presented in Tables I and II.

The map showing the difference in electron density between the thermolysin-inhibitor complex and native thermolysin (Fig. 1) has clear density for the Val-Trp portion of the inhibitor. However, the map does not have positive density close to the zinc at the expected location of the mercaptoacetyl group. This result was unexpected since the sulfur is electron-dense and its location was expected to be obvious in the difference density map. The immediate impression was that the inhibitor had been hydrolyzed with the Val-Trp product remaining bound to the enzyme.

TABLE I

Intensity statistics

$R = \sum|I - \bar{I}|/\sum I$. R_{sym} gives the agreement between symmetry-related reflections measured on the same film. R_{merge} is the agreement between reflections measured on different films.

Number of films	28
Average R_{sym}	3.1%
R_{merge}	4.9%
Average isomorphous difference	10.1%
Total reflections measured	45,350
Independent reflections	28,779
Resolution	1.7 Å
Cell dimensions	
a, b	94.1 Å
c	131.4 Å

TABLE II

Refinement statistics

Resolution limits	10.0–1.7 Å
Initial R factor	22.4%
Final R factor	17.3%
Number of cycles	25
Reflections used	28,604
Number of atoms	2,632
Root mean square deviations from ideality	
Bond lengths	0.016 Å
Bond angles	3.2°
Planarity (trigonal)	0.011 Å
Planarity (other planes)	0.017 Å
Torsional angles (not restrained)	16.6°

Refinement of the enzyme-inhibitor complex was begun with coordinates for the Val-Trp moiety. Difference maps with coefficients of the form ($F_{complex,obs} - F_{complex,calc}$) and ($2F_{complex,obs} - F_{complex,calc}$) were monitored frequently during the course of the refinement. These maps revealed the presence of several water molecules bound in the vicinity of the inhibitor but did not show any density that could be interpreted in terms of the "missing" mercaptoacetyl moiety. Therefore, the high resolution refinement also suggested that the inhibitor had been hydrolyzed.

This hypothesis was tested by examining the binding to thermolysin of the dipeptide L-valyl-L-tryptophan (Sigma). Crystals of thermolysin were soaked for 3 days in a 10 mM solution of Val-Trp in the standard mother liquor. Binding was monitored by calculation of a (0*kl*) difference Fourier projection (Fig. 2*A*). In the thermolysin space group, $P6_122$, this map provides views of the active sites of three different thermolysin molecules, each active site being viewed from a different direction (14). In such a map one would expect to see three peaks at the positions corresponding to the electron-dense sulfur atom. The expected locations of a sulfur liganded to the active-site zinc ion are indicated in the figure, but no significant electron density is seen at these sites. The (0*kl*) map does show clear indications that Val-Trp binds in the vicinity of the active-site cleft. Projection maps as shown in Fig. 2*A* provide limited information and cannot be used to obtain detailed information concerning the location of a bound inhibitor. Such difference maps do, however, provide a sensitive way to compare the binding of one inhibitor with another. Fig. 2*B* shows a difference map with amplitudes of the form ($F_{complex\ 1} - F_{complex\ 2}$), where complex 1 is the complex of thermolysin with HSAc-Val-Trp and complex 2 is the complex of thermolysin with Val-Trp. The absence of features in Fig. 2*B* compared with Fig. 2*A* shows that both inhibitors yield complexes with thermolysin that are very similar if not identical. Specifically, there is no significant positive density close to the three locations expected if the sulfur was present. In terms of the observed structure amplitudes, the average isomorphous difference for Val-Trp bound to thermolysin is 8.5% for the centrosymmetric (0*kl*) data measured to 3.8-Å resolution by precession photography. The average isomor-

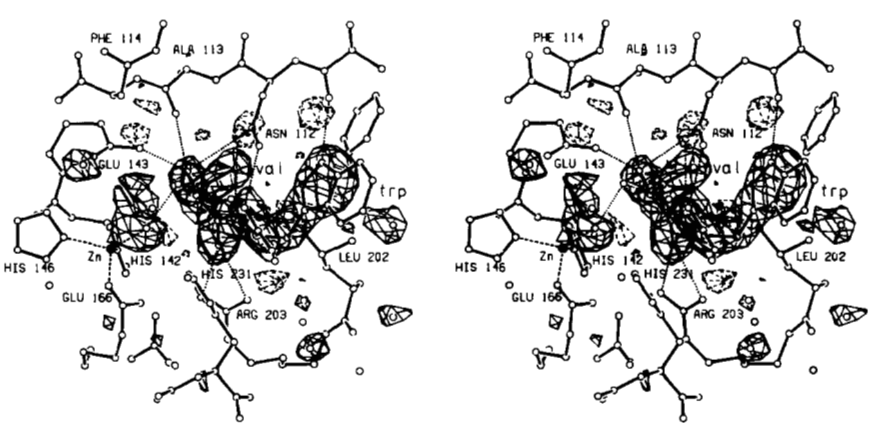

FIG. 1. **Difference map calculated with amplitudes ($F_{complex} - F_c$) where $F_{complex}$ is the observed amplitude for the complex of thermolysin with HSAc-Val-Trp and F_c is the amplitude calculated for the refined structure of thermolysin with solvent molecules removed from the active site.** Phases correspond to F_c. Resolution is 1.9 Å. Positive contours (solid) are drawn at 3σ and negative contours (broken) are drawn at -3σ where σ is the root mean square density throughout the unit cell. The superimposed inhibitor is drawn with *solid bonds* and the protein with *open bonds*. It is believed that the species bound to the enzyme is Val-Trp (see text). The electron density for the distal portion of the indole side chain is weak as has been observed in other complexes of thermolysin with a tryptophan at this position (2, 21).

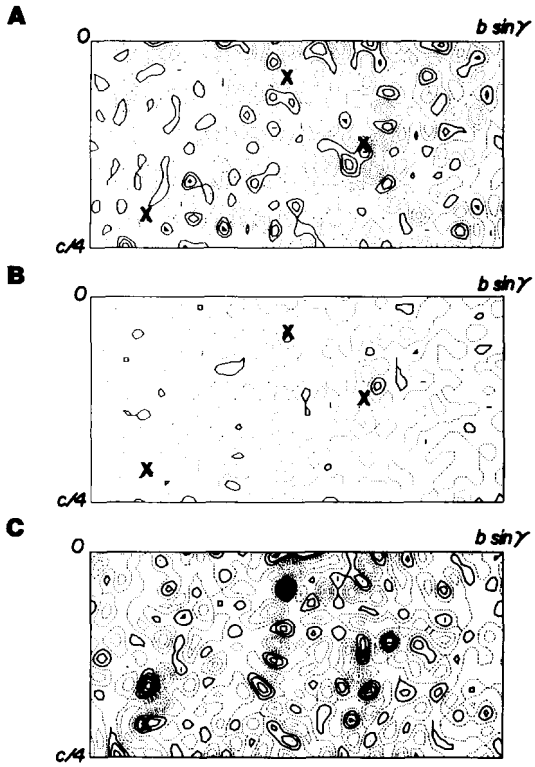

FIG. 2. *A*, projection map showing the difference between the complex of thermolysin with Val-Trp and native thermolysin: amplitudes ($F_{Tln:Val-Trp} - F_{Tln}$); phases determined from isomorphous replacement; resolution 3.8 Å. Positive contours (*solid*) and negative contours (*dotted*) are drawn at arbitrary equal intervals. The three *crosses* indicate the positions where electron density is expected for a sulfur liganded to the active-site zinc. A bound inhibitor is seen three times in this projection, but the electron density in these three views appears dissimilar because the direction of view is different in each case. *B*, projected difference in density between the respective complexes of thermolysin with HSAc-Val-Trp and thermolysin with Val-Trp. Contours are drawn at the same levels as in *A*. *C*, projected difference in density between thermolysin and its complex with *S*-thiorphan (thiorphan: HS-CH_2-CH-($CH_{2\phi}$)-CONH-CH_2-COOH (18)). Coefficients ($F_{Tln:Thiorphan} - F_{Tln}$); otherwise as in *A* (unpublished data of Dr. S. Roderick).

phous difference between the respective inhibitor-enzyme complexes is 4.0% which is essentially equal to the expected error in the precession data. As a further control, Fig. 2*C* shows the projected difference in electron density between thermolysin and its complex with the sulfur-containing inhibitor *S*-thiorphan (*N*-[(*S*)-3-mercapto-2-benzylpropanoyl]glycine) (18).[2] In this instance there is significant positive density at the three expected positions. This map shows that difference Fourier projections as used here to monitor inhibitor binding are clearly able to show the presence of a bound sulfur atom.

Refined coordinates for bound Val-Trp and associated water molecules are given in Table III. The complete set of refined coordinates for the thermolysin-inhibitor complex has been deposited in the Brookhaven Data Bank.

DISCUSSION

Identity of the Bound Inhibitor—There are several lines of evidence that support the identification of the bound inhibitor as Val-Trp rather than HSAc-Val-Trp. First, the electron density of the bound complex strongly supports the identification (Fig. 1). A sulfur atom is electron-dense and should readily be detected even if bound with relatively low occupancy. Fig. 2*C* demonstrates that a bound sulfur can be detected in a medium-resolution Fourier projection. It should be much more obvious in a high-resolution three-dimensional map. The coordinates obtained from the crystallographic refinement, which is to high resolution, are consistent with Val-Trp. In particular, the valyl nitrogen participates in a number of hydrogen bonds with solvent and with the protein (Figs. 3 and 4). This is consistent with a free amino group at this position but would not be expected if a *N*-mercaptoacetyl group were present. Finally, the projection analysis of the binding of Val-Trp suggests that its complex with thermolysin is indistinguishable from that obtained by soaking HSAc-Val-Trp into crystalline thermolysin (Fig. 2*B*).

It will be noted that the *N*-acetyl portion of HSAc-Val-Trp is very similar to a peptide bond. Also, extrapolating from the observed mode of binding of Val-Trp, the amide group is ideally positioned to allow enzymatic cleavage. With hindsight, it is not unreasonable that HSAc-Val-Trp could be hydrolyzed by thermolysin.

Mode of Binding—The specificity of peptide bond cleavage by thermolysin is determined primarily by the amino acid adjacent to and on the COOH-terminal side of the bond to be cleaved. Leucine, isoleucine, and phenylalanine are preferred at this position (19, 20). In contrast, peptides with tryptophan

TABLE III

Inhibitor and solvent coordinates

The coordinates are given in angstroms in the standard orthogonal coordinate system (24). The total number of solvent molecules included in the refined thermolysin-inhibitor complex is 173. Only those in the immediate vicinity of the bound inhibitor are included here. Their identification numbers are essentially arbitrary.

	X	*Y*	*Z*	*B*
	Å	Å	Å	Å²
Val				
N	51.56	18.50	−3.86	12.7
CB	53.15	18.91	−1.89	17.4
CG1	54.61	19.33	−1.65	15.3
CG2	52.56	17.98	−0.82	11.2
CA	52.93	18.40	−3.31	24.2
C	53.75	17.12	−3.58	17.2
O	54.98	17.10	−3.57	14.5
Trp				
N	53.05	16.01	−3.83	12.7
CB	54.09	13.93	−2.91	10.7
CG	52.90	13.45	−2.21	18.0
CD1	52.17	14.18	−1.34	24.5
NE1	51.12	13.42	−0.88	22.8
CE2	51.15	12.19	−1.47	31.2
CZ2	50.30	11.09	−1.33	43.2
CH2	50.61	9.97	−2.07	50.6
CZ3	51.73	9.90	−2.91	45.0
CE3	52.56	11.01	−3.04	50.4
CD2	52.28	12.17	−2.31	31.6
CA	53.67	14.73	−4.13	15.2
C	52.81	13.95	−5.10	28.5
O	51.67	14.44	−5.40	18.8
OH	53.32	12.92	−5.61	31.4
Solvent				
800	58.38	10.39	−0.09	40.7
802	56.89	10.02	−7.04	28.7
803	52.62	11.41	−7.60	33.8
804	55.71	11.60	−5.13	12.1
805	50.68	16.71	−9.17	31.4
806	47.89	29.62	−13.71	43.1
807	50.82	17.31	−6.31	21.9
808	53.66	10.19	−0.22	26.0
809	50.11	13.62	−7.59	44.6
810	53.16	18.67	−6.83	21.3

[2] S. Roderick, B. R. Rogues, and B. W. Matthews, unpublished results.

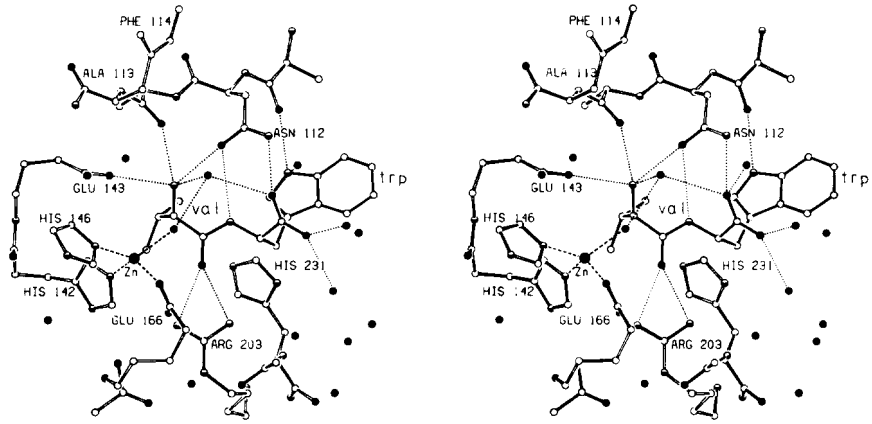

FIG. 3. **Stereo drawing illustrating the mode of binding of Val-trp (*solid bonds*) to thermolysin (*open bonds*).** Presumed hydrogen bonds to the inhibitor are drawn as *dotted lines*; interactions with the zinc are shown as *broken lines*. For clarity, protein-protein and protein-solvent hydrogen bonds are not shown explicitly. Oxygen atoms are drawn *solid*, nitrogen atoms *half-solid*, and carbon atoms are represented by *open circles*.

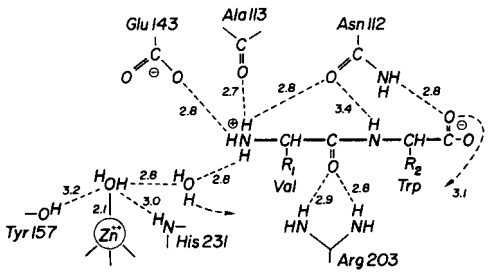

FIG. 4. **Schematic diagram showing the apparent hydrogen bonds (*broken lines*) between Val-Trp and crystalline thermolysin.** The numbers give distances in angstroms. A hydrogen bond between the carboxyl terminus of the dipeptide and a water molecule near the amino terminus is indicated by the *two arrows*.

at this site are very poor substrates. This can be readily understood in terms of the three-dimensional structure of the enzyme (8). The S_1' subsite consists of a hydrophobic pocket that can accommodate side chains such as valine, leucine, and phenylalanine but is too small for a tryptophan side chain. Therefore, the dipeptide Val-Trp cannot occupy the S_1–S_1' subsites. However, a tryptophan can be readily accommodated in the S_2' subsite of thermolysin. Indeed, the tryptophan of the naturally occurring tight-binding inhibitor phosphoramidon (*N*-(α-L-rhamnopyranosyl-oxyhydroxyphosphinyl)-L-leucyl-L-tryptophan) occupies the S_2' subsite (21). Also *N*-(1-carboxy-3-phenylpropyl)-L-leucyl-L-tryptophan), another tight-binding inhibitor (22), binds with tryptophan in the S_2' subsite (2). For such inhibitors, the indole nitrogen donates a hydrogen bond to the backbone carbonyl oxygen of Asn-111. Val-Trp displays the same hydrogen bond (Fig. 3). In summary, the mode of binding adopted by Val-Trp satisfies the specificity requirements of thermolysin in the S_1' subsite and, in addition, has a preferred amino acid in the S_2' position. This mode of binding of a dipeptide to thermolysin is in contrast to Ala-Phe and to the dipeptide analogue β-phenylpropionyl-L-phenylalanine, both of which occupy the S_1-S_1' subsites (8).

Implications for the Mechanism of Action—All inhibitors of thermolysin that have previously been studied crystallographically display a specific interaction with the active-site zinc (Ref. 5 and citations therein). Val-Trp is different in that it occupies the S_1'-S_2' subsites and no part of the inhibitor is in contact with the zinc (Figs. 3 and 4). Because of its mode of binding and also because it has a free amino group, Val-Trp provides a direct crystallographic model for the binding of one of the products of peptide hydrolysis.

The valyl amino group (presumably protonated) appears to make hydrogen bonds to the backbone carbonyl oxygen of Ala-113, the side chain carbonyl oxygen of Asn-112 and a solvent molecule which is in turn hydrogen-bonded to the zinc-bound water (or hydroxide ion) (Figs. 3 and 4). In addition, the valyl nitrogen has a fourth interaction, namely with the carboxylate of Glu-143 (Figs. 3 and 4). This is exactly the interaction that is predicted for the product of a peptide cleaved in the manner suggested by Hangauer *et al.* (3). According to this mechanism of action, the carbonyl oxygen of the peptide bond to be hydrolyzed is liganded to the zinc and displaces a prebound water molecule toward Glu-143. This water molecule, under the combined influence of the zinc ion and Glu-143, attacks the peptide carbonyl carbon to form a tetrahedral transition-state intermediate that is stabilized by interactions with the zinc ion and other groups on the enzyme including His-231 and Tyr-157. The proton that is abstracted by Glu-143 from the attacking water molecule is then transferred to the nitrogen of the scissile peptide bond leading to breakage of the bond and subsequent release of products. The postulated mechanism requires that Glu-143 can initially help promote the nucleophilic attack of the zinc-bound water on the carbonyl carbon of the substrate. This aspect of the proposed mechanism is supported by prior structural studies of presumed transition-state analogues (2–5, 23). The mechanism also requires that Glu-143 can be close enough to the nitrogen of the scissile bond to transfer the proton that is abstracted from the nucleophilic water molecule. This was suggested by the modes of binding of presumed transition-state analogues but was not observed directly (2–5). The present analysis is the first instance in which a direct interaction between Glu-143 and the nitrogen of the scissile bond has been seen in a thermolysin-inhibitor complex. While the nitrogen is close (2.8 Å) to OE2 of Glu-143, it is much further (5.2 Å) from NE2 of His-231. This tends to support Glu-143 as the proton donor in catalysis rather than His-231. The present analysis does not, however, exclude water as a possible proton donor.

Notwithstanding the above discussion it must be emphasized that mechanistic arguments based on structural complexes of enzyme-inhibitor complexes are essentially indirect. One cannot be sure that a static complex represents a true catalytic intermediate. It could be that the protonated amino group of the present inhibitor interacts with Glu-143 just because this is the most favorable geometry that happens to be available. However, in the absence of conflicting evidence we believe that it is legitimate to use appropriate enzyme-inhibitor complexes to visualize the likely configurations of intermediates in catalysis.

Acknowledgments—We are grateful to Dr. Miguel A. Ondetti for helpful suggestions and advice concerning inhibitors of thermolysin

and for gifts of such inhibitors. We also thank Dr. D. E. Tronrud for help with computing and preparation of the figures and Dr. S. Roderick for providing Fig. 2*C*.

REFERENCES

1. Kester, W. R., and Matthews, B. W. (1977) *J. Biol. Chem.* **252,** 7704–7710
2. Monzingo, A. F., and Matthews, B. W. (1984) *Biochemistry* **23,** 5724–5729
3. Hangauer, D. G., Monzingo, A. F., and Matthews, B. W. (1984) *Biochemistry* **23,** 5730–5741
4. Tronrud, D. E., Monzingo, A. F., and Matthews, B. W. (1986) *Eur. J. Biochem.* **157,** 261–268
5. Holden, H. M., Tronrud, D. E., Monzingo, A. F., Weaver, L. H., and Matthews, B. W. (1988) *Biochemistry*, in press
6. Gardell, S. J., Craik, C. S., Hilvert, D., Urdea, M. S., and Rutter, W. J. (1985) *Nature* **317,** 551–554
7. Christianson, D. W., David, P. R., and Lipscomb, W. N. (1987) *Proc. Natl. Acad. Sci. U. S. A.* **84,** 1512–1515
8. Kester, W. R., and Matthews, B. W. (1977) *Biochemistry* **16,** 2506–2516
9. Schechter, I., and Berger, A. (1967) *Biochem. Biophys. Res. Commun.* **27,** 157–162
10. Monzingo, A. F., and Matthews, B. W. (1982) *Biochemistry* **21,** 3390–3394
11. Ondetti, M. A., Condon, M. E., Reid, J., Sabo, E. F., Cheung, H. S., and Cushman, D. W. (1979) *Biochemistry* **18,** 1427–1430
12. Holmquist, B., and Vallee, B. L. (1979) *Proc. Natl. Acad. Sci. U. S. A.* **76,** 6216–6220
13. Ondetti, M. A., Cushman, D. W., Sabo, E. F., Natarajan, S., Pluscec, J., and Rubin, B. (1981) in *Molecular Basis of Drug Action* (Singer, T. P., and Ondarza, P. N., eds) pp. 235–246, Elsevier/North-Holland, New York
14. Matthews, B. W., Jansonius, J. N., Colman, P. M., Schoenborn, B. P., and Duporque, D. (1972) *Nature* **238,** 37–41
15. Schmid, M. F., Weaver, L. H., Holmes, M. A., Grutter, M. G., Ohlendorf, D. H., Reynolds, R. A., Remington, S. J., and Matthews, B. W (1981) *Acta Crystallogr. Sect. A Cryst. Phys. Diffr. Theor. Gen. Crystallogr.* **37,** 701–710
16. Jones, T. A. (1982) in *Crystallographic Computing* (Sayre, D., ed) pp. 303–317, Oxford University Press, Oxford
17. Tronrud, D. E., Ten Eyck, L. F., and Matthews, B. W. (1987) *Acta Crystallogr. Sect. A Cryst. Phys. Diffr. Theor. Gen. Crystallogr.* **43,** 489–501
18. Roques, B. R., Fournie-Zaluski, M. C., Soroca, E., Lecomte, J. M., Malfroy, B., Llorens, C., and Schwartz, J. C. (1980) *Nature* **288,** 286–288
19. Matsubara, H., Sasaki, R., Singer, A., and Jukes, T. H. (1966) *Arch. Biochem. Biophys.* **115,** 324–331
20. Morihara, K., Tsuzuki, H., and Oka, T. (1968) *Arch. Biochem. Biophys.* **123,** 572–588
21. Weaver, L. H., Kester, W. R., and Matthews, B. W. (1977) *J. Mol. Biol.* **114,** 119–132
22. Maycock, A. L., DeSousa, D. M., Payne, L. G., ten Broeke, J., Wu, M. T., and Patchett, A. A. (1981) *Biochem. Biophys. Res. Commun.* **102,** 963–969
23. Holmes, M. A., and Matthews, B. W. (1981) *Biochemistry* **20,** 6912–6920
24. Matthews, B. W., Weaver, L. H., and Kester, W. R. (1974) *J. Biol. Chem.* **249,** 8030–8044